Desalination and Water Treatment
www.deswater.com
doi: 10.5004/dwt.2019.23169

137 (2019) 101–113
January

Effect of operational variables on biological hydrogen production from palm oil mill effluent by dark fermentation using response surface methodology

Azam Akhbari[a], Ali Akbar Zinatizadeh[b,c], Mohsen Vafaeifard[a], Parviz Mohammadi[d], Bidattul Syirat Zainal[a], Shaliza Ibrahim[a,*]

[a]*Department of Civil Engineering, Faculty of Engineering, University of Malaya, Kuala Lumpur, Malaysia, emails: Shaliza@um.edu.my (S. Ibrahim), aazam.akhabri@yahoo.com (A. Akhbari), Mohsen.vafaeifard@gmail.com (M. Vafaeifard), syirat88@gmail.com (B.S. Zainal)*
[b]*Department of Applied Chemistry, Faculty of Chemistry, Razi University, Kermanshah, Iran, email: zinatizadeh@gmail.com*
[c]*Environmental Research Center (ERC), Department of Applied Chemistry, Faculty of Chemistry, Razi University, Kermanshah, Iran*
[d]*Research Center for Environmental Determination of Health (RCEDH), Kermanshah University of Medical Sciences, Kermanshah, Iran, email: parviz8855@yahoo.com*

Received 8 April 2018; Accepted 15 September 2018

ABSTRACT

This work is a study of the performance and effect of operational parameters on biohydrogen production from palm oil mill effluent by dark fermentation in batch mode. The tests were conducted with samples prepared in 150 mL bottles using a shaker at 150 rpm. Response surface methodology was applied to investigate the influence of the four significant independent parameters viz. pH (5, 5.5, and 6), temperature (30°C, 35°C, and 40°C), substrate concentration (5,000, 12,500, and 20,000 mg L^{-1}) and inoculum–substrate ratios of 2, 0.8, and 0.5 (expressed as volatile suspended solid (VSS) basis) with the inoculum concentration of 10 g L^{-1} VSS on biohydrogen production. All the experiments were analyzed at the incubation time of 8, 16, and 24 h. Upon seeing each interval, the results were compared. The highest chemical oxygen demand (COD) removal, the hydrogen content in the biogas as hydrogen percentage (H_2%), and hydrogen yield (HY) were obtained 58.3%, 80%, and 3.63 mol H_2 mol^{-1} glucose, respectively, at 24 h incubation time. An overlay study was done to find an overall optimization of the parameters. The optimized conditions were COD removal 49%, HY 3.2 mol H_2 mol^{-1} glucose, and hydrogen percentage 80%. Also, the Monod model was studied to calculate the kinetics constants of the maximum substrate utilization rate (U_{max}) and half-velocity K_s which are found to be 0.261 g L^{-1} d^{-1} and 0.349 mg L^{-1}, respectively.

Keywords: Biological treatment; Hydrogen production; Dark fermentation; Chemical oxygen demand removal; Monod model

1. Introduction

One of the most vital environmental concerns is how to achieve new renewable energy from organic sources. Renewable energy is a great alternative to fossil fuels and protects the environment. Fossil fuel usage is a severe environmental concern today because greenhouse gas pollutant emissions cause extreme global climate changes. Accordingly, various studies have been done recently to identify sustainable sources of energy with no adverse impacts on the environment [1]. Biohydrogen is deliberated as a remarkable prospect clean energy carrier because of its environment-friendly conversion, high energy content and also can be produced by less energy-intensive processes [1]. Hydrogen fuel due to the elimination of entirely environmental problems that are produced by the fossil is evaluated as a promising alternative source of energy compared with the conventional methods [2]. Hence, biological hydrogen production in comparison with conventional physicochemical methods

* Corresponding author.

is conceivably a sustainable greener technology which falls into three general groups: solar conversion, electrolysis, and biomass conversion [3,4].

Malaysia is one of the prominent producers of palm oil mill effluent (POME) in the world with approximately 50 million tons' production per year [5]. POME is characterized by high organic acid content, carbohydrate, minerals, and proteins which make this waste source as a suitable nutrient for biomass growth and consequently substrate for hydrogen production [6].

Numerous approaches have been applied to investigate biohydrogen produced via dark anaerobic fermentation using a range of renewable sources as substrate [7,8]. Recently, dark fermentation (DF) has achieved increased attention, mainly due to high production rate with low energy consumption, flexibility in the use of a wide range of carbohydrate concentration which makes it more practical technology compared with photosynthesis process [7,9,10]. The dark hydrogen production is done by fermentative hydrogen-producing microorganisms which are cultivated in anaerobic conditions. The organic compounds are broken down by these microorganisms as carbon and energy source to provide the energy for the microorganism's metabolisms, this process is defined as dark hydrogen fermentation [11].

The process of DF via batch mode is complicated as some parameters including inoculum acclimatizing such as substrate types, enrichment, pretreatment, and environmental parameters optimization including temperature, pH, and substrate concentration can regulate and affect the metabolic pathway of microorganisms which produce hydrogen [10]. By developing hydrogen production, the accumulation of acids with higher molecular weight such as acetic and butyric acids occurs in the system. If pH does not control in the appropriate range, it will confine microorganisms from growing and halt the hydrogen production. Also, substrate concentration is a significant parameter that needs to be studied in this process as the high levels might have direct inhibitory influence, or incidentally causing a pH drop due to organic acids accumulation which can initiate a shift in the metabolic pathway of the acetogenesis. Moreover, the impact of temperature on this process has been studied in the mesophilic range. Therefore, it is essential to monitor the essential factors to maintain the hydrogen production. Hence, these parameters are considered necessary to balance the reaction efficiency and the degree of substrate metabolism [12,13]. Moreover, to overwhelm the unfavorable effect of hydrogen-consuming bacteria (HCB) in the processes which result in low hydrogen yield (HY), pretreatment of inoculum sludge to control hydrogen-producing bacteria (HPB) is indispensable [14,15]. According to the literature studies, several pretreatment approaches have been used to halt the HCB including chemical treatment [16], ultraviolet [17], thermal treatment [18], and pH stress (acid or alkaline treatment) [19]. Statistical modeling is a widely employed, useful tool that provides a better understanding of how different variables can affect biological processes. Response surface methodology (RSM) has been recognized as an efficient method to evaluate the optimal conditions [20]. It considers statistical approaches for experimental design, examining the effect of experimental factors, and probing for the optimum conditions. The advantage of using RSM is to eliminate the test run numbers to evaluate several parameters and interactions. Moreover, this less time-consuming method is capable of studying the several factors simultaneously [21,22]. Several researchers examined the optimization and the effect of different crucial parameters on the POME treatment using RSM. According to the theory of this methodology, some experiments were designed and analyzed statistically [23–25]. Therefore, the goal of this work is to consider the application of the RSM on hydrogen production from POME and identify the best estimation of the operational variables affecting this process by DF. Also, the Monod model was studied to calculate the kinetic parameters for considering the organic removal rate.

2. Materials and methods

2.1. Acclimatization of sludge and substrate characterization

The POME sludge was taken from the anaerobic pond at 9 d sludge age and collected from Jugra Palm Oil Mill Sdn. Bhd, Banting, Selangor, Malaysia. The sludge was first sieved through 1 mm mesh size to remove sand and coarse particles. It was then heated at 80°C for 50 min to inactivate the hydrogenotrophic methanogens and enrich it for the HPB [26]. Before transferring the heated sludge into bottles, it was cooled down to room temperature. The characteristics of the anaerobic sludge used were: pH = 7.8 ± 0.1, total suspended solids = 35 g L^{-1}, and volatile suspended solids (VSS) = 10.0 g L^{-1}.

The collection location for substrate (POME) was same with POME sludge. It was collected from the pond after the acidification process. After collecting, the samples were kept in a cold room at 4°C. The samples were allowed to be settled before using due to the high amounts of suspended solids. Hence, the supernatant was used as a substrate known as presettled POME. The POME substrate with chemical oxygen demand (COD) concentration of 50,000 ± 2,000 was diluted to prepare the three different COD concentrations of the 5,000, 12,500, and 20,000 mg L^{-1}. The chemical characteristics of the presettled POME used in this study are compared and provided in Table 1.

2.2. Experimental apparatus and procedure

Batch tests were done in a set of 150 mL serum bottles, and the operating volume was 100 mL for each batch of fermentation solution. The pretreated sludge ((10 g L^{-1} VSS; substrate concentration (5,000, 12,500, and 20,000 mg L^{-1}) (inoculum–substrate ratios (ISRs) 2, 0.8, and 0.5 (expressed as VSS basis)) were added into a 150 mL serum bottle. Then the bottles were stirred at 150 rpm to cultivate hydrogen-producing mixed bacteria at three different temperatures (30°C, 35°C, and 40°C).

The pH was adjusted in three different ranges (5, 5.5, and 6). The concentrations of COD, total Kjeldahl nitrogen (TKN), pH, mixed liquor suspended solids, VSS, oil and grease (O&G), total solids, total volatile solids, and NH_3-N of the system were measured by using standard methods for examining water and wastewater [27]. For COD, a colorimetric method with a closed reflux technique was used. A spectrophotometer (pharo 100, Merck, Perkin Elmer) at 600 nm was used to measure the absorbance of the COD samples.

Table 1
Characterization of palm oil mill effluent (POME)

Parameter	Concentration				
Temperature (°C)	80–90	–	–	–	80–90
pH	4.7	6.4	5–9	4–5	5 ± 0.2
Oil and grease (O&G) (mg L^{-1})	4,000	2,100	2,500–10,000	8,100–10,500	4,000 ± 20
Biochemical oxygen demand (BOD) (mg L^{-1})	25,000	51,510	11,000–45,000	22,100–54,200	25,000 ± 1,000
Chemical oxygen demand (COD) (mg L^{-1})	50,000	49,500	>80,000	75,100–96,300	50,000 ± 2,000
Total solid (TS) (mg L^{-1})	40,500	36,700	–	35,000–42,000	40,000 ± 1,000
Total suspended solid (TSS) (mg L^{-1})	18,000	13,300	–	8,400–12,000	18,000 ± 500
Total volatile solid (TVS) (mg L^{-1})	34,000	–	34,000	–	34,000 ± 800
NH_3-N (mg L^{-1})	35	–	35	25–30	35 ± 1
TKN (mg L^{-1})	750	–	750	820–910	750 ± 5
Turbidity (NTU)	–	–	–	–	664 ± 4
Ref.	[27]	[28]	[29]	[30]	This study

The TKN was determined by a TKN meter Gerhardt model (vapodest 10). A pH meter model EUTEC INSTRUMENTS Ph700 was used to measure the pH. Turbidity was measured by a YSI ProDSS 4-port digital sampling system, USA. A shaker incubator (lab trc, Daihan Iabtec Co., Ltd.) was used for incubation. For alkalinity, 2,000 mg L^{-1} $NaHCO_3$ was added to each bottle. The pH was adjusted with NaOH (4 M) and HCl (2 M). The bottles were sparged with nitrogen (N_2) gas for 3 min to create an anaerobic condition, after which they were sealed with silicone rubber. The water displacement method was used to record the volume of biogas produced. The biogas was analyzed by gas chromatography equipped with a thermal conductivity detector (TCD, Perkin Elmer, Auto System Gas Chromatograph, 600 Series LINK), a pack GC column Supelco, 40/80 carboxen 1000, MR2924D, 10′ × 1.8′ was used to analyze the biogas composition. The high purity argon gas at a flowrate of 30 mL min^{-1} was used as carrier gas. The temperature was adjusted to 100°C, 150°C, and 200°C for the oven, injector, and detector, respectively. A 0.5 mL gas tight syringe 2,500 mL Hamilton, USA was used for gas sampling for injection determinations. The biogas products detected were only hydrogen, nitrogen, and carbon dioxide gas.

2.3. Design of experiments

The Design Expert Software (Stat-Ease Inc., version 6.0.6) was applied for the experimental design and data analysis. RSM and central composite design were used to optimize the operating variables. The four effective variables, that is, initial pH (*A*), temperature (*B*), substrate concentration (*C*), and ISRs (*D*) were used to determine the responses for the biohydrogen production amounts. The variable ranges selected were (5,5.5, and 6), (30°C, 35°C, and 40°C), (5,12.5, and 20 g L^{-1}), and (2, 0.8, and 0.5) for *A*, *B*, *C*, and *D* parameters, respectively. The full face-centered experimental design was used to evaluate the batch test performance in biohydrogen production. The design is comprised of 2*k* factorial points developed from a center point and 2*k* axial points, where *k* represents the variables number. Three levels including low (−1), central (0), and high (+1) were used to measure the variables. Therefore, 30 experiments (=2*k* + 2*k* + 6, where *k* is the factors number) were performed with 25 tests organized in a factorial design (including 16 factorial points, 8 axial points, and 1 center point) [20]. The residuals five runs concerning the central point repetition also designed to provide an adequate estimation of the experimental error was designed as well. Hence, to achieve a complete analysis, dependent parameters including COD removal, hydrogen percentage, and HY were also measured as the response.

2.4. Mathematical modeling and statistical analysis

The statistical analysis was carried out to assess the RSM model. Subsequently, to evaluate the interactive and individual influence of parameters on the response, the analysis of variance (ANOVA) was applied to deduce the results. This can be performed more efficiently if the results are interpolated and the error is removed by changing one factor and repeating the runs. Three categories of tests were run, including regression modeling, the significance of terms, and lack-of-fit. These experiments assess the importance and design consistency. Moreover, ANOVA was used to assess the results with Design-Expert software, and results are provided in Table 2 accordingly. Higher degree polynomial equations were used to quantify the effect of the curvatures. Three-dimensional plots and corresponding predicted versus actual plots according to the influence of two factors level were obtained as well. The experimental results are provided in Table 3 as well.

The more dynamic variables are determined by the importance of terms, which depends on the probability value (*p*-value). The *p*-value ascertains the closeness of the obtained results to the actual experimental data and within and across the model variables. The *p*-value also affects the response variables, whereby a smaller *p*-value means the variable has a significant effect on the response. A *p*-value lower than 0.05 indicates the model is significant when it is quadratic. To assess the experimental data precision, a regression model (R^2) was used, which considers the regression coefficient (R^2) and the adjusted regression coefficient (Adj-R^2) values. The R^2

Table 2
ANOVA results for the equations of the Design Expert 6.0.6 for studied responses

Response	Time (h)	Modified equations with significant terms	Probability	R^2	Adj. R^2	Adeq. precision	SD	CV	PRESS	Probability for lack of fit
COD removal	8	$+16.47 + 1.00 \times A + 2.18 \times B + 1.19 \times C + 0.21 \times D + 2.56 \times AD$	<0.0001	0.84	0.708	10.309	1.46	9.04	180.02	0.294
	16	$+35.92 + 1.76A + 4.35 \times B + 1.5 \times C + 1.38 \times D + 4.64 \times A^2 - 8.04 \times B^2 + 2.39 \times A \times D$	<0.0001	0.84	0.772	11.720	2.98	8.81	461.20	0.31
	24	$+49.31 + 1.38 \times A + 4.98 \times B + 1.24 \times C + 0.49 \times D - 8.92 \times B^2 + 3.12 \times D^2 + 1.80 \times A \times C$	<0.0001	0.92	0.892	19.357	1.98	4.31	213.15	0.080
Hydrogen percentage	8	$+39.66 + 1.81 \times A + 5.54 \times B + 0.77 \times C + 0.89 \times D - 2.68 \times B^2 + 3.43 \times C^2 + 0.53 \times C \times D$	<0.0001	0.78	0.579	8.423	3.74	9.45	228.94	0.385
	16	$+78.44 + 5.84 \times A + 4.52 B - 1.21 \times C + 3.64 \times D - 11.17 \times A^2 + 20.50 \times B^2$	<0.0001	0.84	0.693	7.999	8.49	13.33	389.48	0.498
	24	$+87.29 + 4.30 \times A + 9.47 \times B + 3.02 \times C + 0.84 \times D - 6.90 \times A^2 + 29.81 \times B^2 + 0.11 \times A \times B$	<0.0001	0.97	0.972	32.374	3.29	5.04	486.54	0.113
Hydrogen Yield	8	$+1.04 + 0.11 \times A + 0.059 \times B - 0.52 \times C + 0.063 \times D + 0.29 \times A^2 - 0.27 \times B^2 + 0.067 \times C^2 + 0.31 \times D^2 + 0.049 \times A \times C$	<0.0001	0.85	0.577	5.512	0.37	23.77	5.51	0.231
	16	$+4.71 + 0.15 \times A - 0.23 \times B - 0.88 \times C + 0.45 \times D + 7.01E{-}004 \times A^2 - 0.64B^2 + 0.44 \times C^2$	<0.0001	0.82	0.537	5.273	0.61	13.98	214.55	0.54
	24	$+3.23 + 0.05 \times A + 0.34 \times B - 0.63 \times C + 0.5 \times D + 0.33 \times A^2 + 0.12 \times B^2 + 5.625E{-}003 \times A \times C$	<0.0001	0.88	0.538	7.336	0.59	18.69	279.63	0.92

value ranged from 0 to 1. Thus, a model with a value of 1 is an ideal one which shows a significant impact on the response. Further, the Adj-R^2 coefficient provides a more accurate indication of the fitting of the model. Its value declined by adding of the nonsignificant term in comparison with an R^2 value which improved by increase of the new term [28]. The model adequacy was examined through lack-of-fit *F*-tests [29]. Adequate precision is a signal to noise ratio or is considered as a degree of the range in projected response about its related error. An ideal value is 4 or more [30]. In this study, the value was found to be appropriate for all models. The plot of predicted versus actual responses is shown in Fig. 1.

2.5. Mass balance-based (Monod) model

Some kinetic models are used for substrate removal such as Monod, Grau first and the second model, Chan-Hashimoto, Contois, zero-, first- and second-degree, improved Stover–Kincannon. In this study, the substrate utilization rate was modeled by this model at three incubation time of 8, 16, and 24 h to study the kinetic equations. However, the results of the incubation time of 24 h are presented in Table 3. Nutrient removal rate in a batch reactor is recognized as Eq. (1) by Monod kinetics model [31].

$$\frac{ds}{dt} = U = \frac{k_{max} \times X \times S}{K_s + S} \tag{1}$$

It is assumed that X is constant and $k_{max} \times X$ considered as U_{max}, by the initial condition ($S = S_0$ in $t_0 = 0$) and making integration, Eq. (1) can be rewritten as follows [32]:

$$\frac{1}{U} = \frac{K_s}{U_{max}} \times \frac{1}{S} + \frac{1}{U_{max}} \tag{2}$$

where U is substrate consumption rate (g L^{-1} d^{-1}), U_{max} is maximum substrate utilization rate (g $L^{-1}d^{-1}$), S is substrate concentration(g L^{-1}), and K_s (g L^{-1}) is half-velocity constant, known as the microorganisms affinity to the substrate. K_s can be considered as a process efficiency indicator; high values of the constant propose low system efficiency. From Eq. (2), the values of U_{max} and K_s can be attained by plotting ($1/U$) versus ($1/S$). These coefficients can be calculated from the intercept and the slope of the straight line, respectively.

3. Results and discussion

3.1. COD removal

The response dependency on the operational variables was modeled to define the impact of different parameters on COD removal efficiency. According to Table 2, a quadratic model was selected to analyze the response. The regression equation shows an empirical model with coded factors for COD removal. The ANOVA results in Table 2 indicate that the model can be used to cross the design space. Hence, to recommend a model, a plot of predicted versus actual values was provided by Design-Expert software (ver. 6.0.7) to judge the model's adequacy. In Fig. 1, the R^2 and adjusted R^2 values indicate that there is an acceptable relationship between the predicted and actual data. Also, the *F*-value

Table 3
Experimental conditions and results of central composite design at incubation time = 24 h

Variables					Responses		
Run no.	pH	Temperature (°C)	Substrate concentration (mg L^{-1})	ISR	COD removal (%)	H_2 percentage	Hydrogen yield (mol H_2 mol^{-1} glucose)
1	6.00	30.00	5,000.00	2.0	35.46	45.76	3.26
2	5.50	35.00	12,500.00	0.8	48.02	84.52	3.32
3	5.00	30.00	20,000.00	0.5	35.78	36.89	1.01
4	5.50	35.00	12,500.00	0.8	51.24	86.12	2.63
5	5.00	40.00	20,000.00	0.5	46.23	62.96	2.63
6	5.50	35.00	12,500.00	0.8	49.32	88.16	2.69
7	5.00	40.00	5,000.00	2.0	46.75	45.93	3.46
8	6.00	40.00	5,000.00	2.0	47.89	57.58	3.42
9	5.50	35.00	12,500.00	0.8	48.75	86.83	2.7
10	6.00	40.00	5,000.00	2.0	58.32	64.19	3.63
11	5.50	30.00	12,500.00	0.8	32.91	55.39	3.29
12	6.00	35.00	12,500.00	0.8	52.05	84.02	3.82
13	5.00	40.00	20,000.00	0.5	47.87	60.38	3.02
14	5.00	30.00	5,000.00	2.0	39.60	36.09	3.17
15	6.00	30.00	20,000.00	0.5	39.87	42.87	2.10
16	5.50	35.00	20,000.00	0.5	48.96	85.27	2.72
17	5.50	40.00	12,500.00	0.8	45.43	63.67	3.32
18	6.00	30.00	20,000.00	0.5	35.23	46.99	1.92
19	6.00	40.00	20,000.00	0.5	50.19	70.94	2.41
20	5.50	35.00	12,500.00	0.8	48.02	84.52	3.12
21	5.50	35.00	12,500.00	0.8	49.00	83.89	2.82
22	5.50	35.00	5,000.00	2.0	49.46	87.31	3.28
23	5.00	35.00	12,500.00	0.8	48.08	80.85	3.32
24	6.00	40.00	20,000.00	0.5	50.37	71.24	2.65
25	5.50	35.00	12,500.00	0.8	50.26	90.12	3.20
26	5.00	30.00	20,000.00	0.5	32.78	38.57	2.43
27	5.00	40.00	5,000.00	2.0	46.17	50.53	3.48
28	5.00	30.00	5,000.00	2.0	43.60	34.17	2.81
29	6.00	30.00	5,000.00	2.0	48.32	40.19	3.15
30	5.50	35.00	12,500.00	0.8	50.12	89.00	2.91

shows the lack of fit is not significant corresponding to the clear error. Moreover, it is realized from an insignificant lack of fit (probability value) that the model fits the data well. Figs. 2(a)–(c) contains the plots of the model for COD removal variation as a function of pH and ISR at three different incubation time of 8, 16, and 24 h.

From the study, the effect of pH (*A*) and the substrate to inoculum ratios (*D*) found to be a significant parameter in COD removal efficiency and other insignificant terms were eliminated to simplify the model. As can be seen from ANOVA results for the equations in Table 2, the main-order, multiple-interaction of *A* and *D* and two-level interaction of *D* shows the positive impact on the removal efficiency, while the effect of *B* is insignificant and shows negative impact in two-level interaction. Three-dimensional plots based on the model equation for the measured responses were formed to obtain a better consideration of the variables affect interaction on COD removal efficiency (Table 2).

From Figs. 2(a)–(c), almost the same patterns were found, but more COD removal efficiency achieved with an increase in incubation time from 8 to 24 h. From the plots, COD removal improved slightly with an increase in pH and decrease in ISR. The analysis of three-dimensional plots shows an elongation diagonally in both directions. This indicated that the interaction of pH and ISR was significant which can be confirmed by the ANOVA results accordingly (Table 2).

From the literature, Tao et al. [33] used various wastewater for H_2 production in photo-fermentation condition and achieved over 80% COD removal efficiency. Mishra et al. [34] performed COD removal of 57% from POME in DF stage which followed by 93% removal in photo-fermentation process. Eroğlu et al. [35] used olive mill wastewater as a carbon source for photo-fermentation and gained a maximum COD removal efficiency of 40%. In this study, the maximum COD removal efficiency was obtained 58.32%, 43%, and 21% with the corresponding variables of incubation

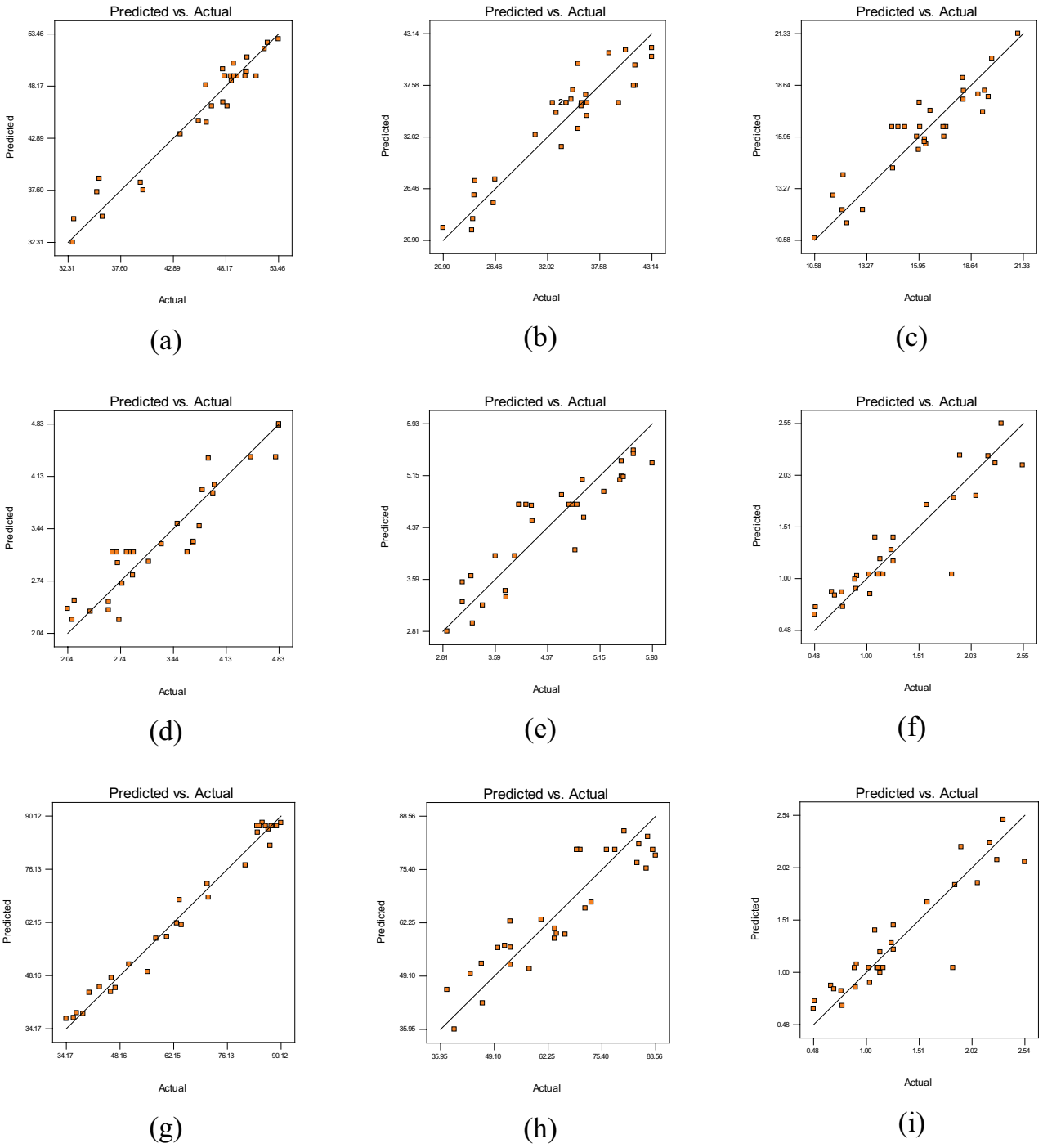

Fig. 1. Design-Expert plot: predicted vs actual values at 24, 16, and 8 h for (a) $R^2 = 0.92$ and Adj-$R^2 = 0.892$, (b) $R^2 = 0.84$ and Adj-$R^2 = 0.772$, and (c) $R^2 = 0.7$ and Adj-$R^2 = 0.694$ (COD removal); (d) $R^2 = 0.7$ and Adj-$R^2 = 0.652$, (e) $R^2 = 0.63$ and Adj-$R^2 = 0.558$, and (f) $R^2 = 0.75$ and Adj-$R^2 = 0.689$ (Hydrogen yield); (g) $R^2 = 0.97$ and Adj-$R^2 = 0.972$, (h) $R^2 = 0.78$ and Adj-$R^2 = 0.722$, (i) $R^2 = 0.7$ and Adj-$R^2 = 0.641$ (Hydrogen percentage).

time 24, 16, and 8 h, pH 6 and substrate concentration of 5,000 mg L^{-1} (ISR 2), respectively. The highest COD removal efficiency was achieved at the lowest COD concentration (the highest ISR value). At higher substrate concentration less removal efficiency was obtained. It means that when the ISR declined from 2.0 to 0.5, presenting the event of an inhibition occurrence by substrate concentration [36]. This response reduction may be due to the mineralization of components into H_2O and CO_2 present in POME, while the increase in COD removal could be due to the formation of simple intermediates gained from the conversion of complex components in POME. [37] At the three reaction temperatures (30°C, 35°C,

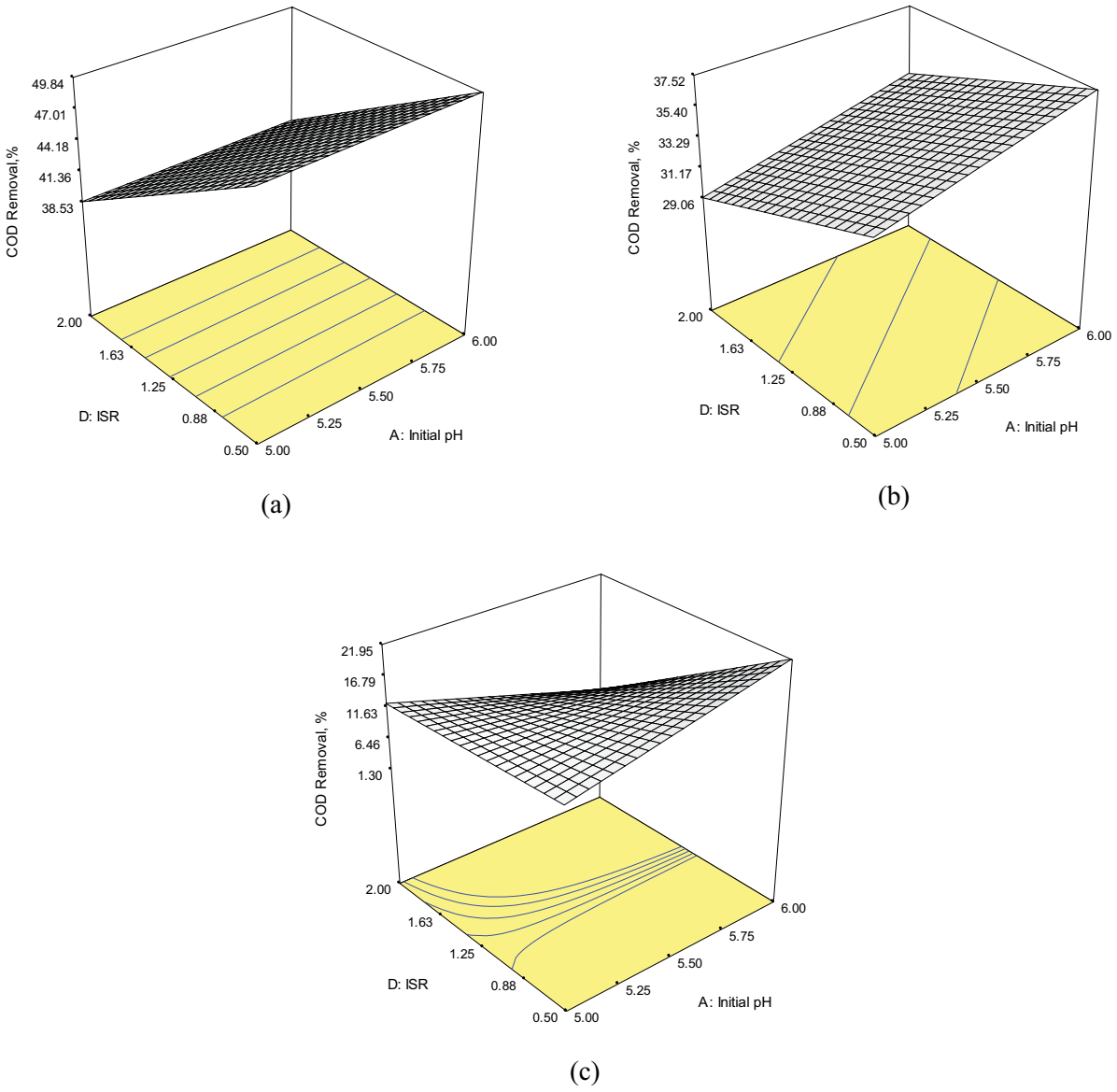

Fig. 2. Three-dimensional plots for COD removal at (a) 24 h, (b) 16 h, and (c) 8 h.

and 40°C), there was no significant COD removal difference, and the range was below 10% at each incubation time [38]. In the test runs that the lowest substrate concentration was used (5,000 mg L^{-1}), a suitable condition that is prepared by $NaHCO_3$ (2,000 mg L^{-1}) which was adequate for maintaining the pH unchanged and suitable for microorganism growth and hydrogen production. Hence, higher substrate concentration and lower pH had a reductive effect on COD removal. Therefore, the minimum response value obtained was 32.78% (pH 5, temperature 30°C, substrate concentration 20,000 mg L^{-1}, and ISR = 0.5) [39].

3.2. Effect of operating variables on hydrogen percentage and hydrogen yield

Hydrogen is evaluated as a source of energy for the future. Nevertheless, from a practical and economic perspective, there are many obstacles. Many research works have examined the effect of various parameters on HY [40,41]. This critical parameter expresses the process efficiency, that is, the quantity of hydrogen produced per amount of substrate consumed [42]. The model terms, *A*, *B*, *C*, and *D* and interaction of *A* and *B* are considered as significant factors while the most effective parameters are found to be *A* and *B*. The three-dimensional based on the model equation were generated as a function of pH (*A*) and temperature (*B*) (Table 2). In this study the pH and temperature (*A* and *B*) range were selected 5, 5.5, and 6, and 30°C, 35°C, and 40°C, respectively. For incubation time of 8 and 16 h, a cubic model was used to analyze the effective parameters and the modified quadratic model was chosen to explain the response variations for incubation time 24 h from the analysis in Table 2. The regression equation is given in this table as well.

One of the most significant parameters affecting hydrogen production is pH (*A*). Several studies concerning the influence of pH on hydrogen production have shown that the optimum pH range to attain the highest hydrogen percentage is between 5.2 and 6.0 [43]. Another factor that affects how microbes produce hydrogen is temperature (*B*) [44,45].

In these experiments, the components of generated biogas were H_2 and CO_2, N_2, and without CH_4 detection. From Fig. 3, the effect of temperature and pH on hydrogen percentage showed that the response increases with increasing the variables from 42% at 8 h to 80% at 24 h. At first 8 h, maximum H_2 percentage obtained at 39°C and pH 5.5, while over incubation time of 16 and 24 h, the highest amount achieved in pH and temperature 5–5.5 and 36°C–38°C, respectively. Hence, increasing the temperature from 30°C to 40°C improved the H_2 percentage [46].

The HY was measured by dividing the total hydrogen production volume by the consumed COD. From the analysis, a higher degree model (cubic model) to improve the R^2 value was used to predict the HY. The plots are shown in Fig. 4 as a function of substrate concentration (*C*) and pH (*A*) at three incubation times. The corresponding areas of plots indicate that the highest HY could be obtained enclosed the studied range of variables. As seen in Fig. 4, it is noted an increase in substrate concentration seems to prevent hydrogen production, which is followed by a reduction in HYs. Hence, the increase in HY has been perceived as the *C* decreased from 20,000 to 5,000 mg L^{-1}. Moreover, at the initial incubation time of 8 h, the lowest HY of 1.6 mol H_2 mol^{-1} glucose was obtained. It was found that as the incubation time increased to 24 h, HY is increased as well which shows the significant effect of this parameter on the response. The maximum HY of 3.63 mol H_2 mol^{-1} glucose was obtained

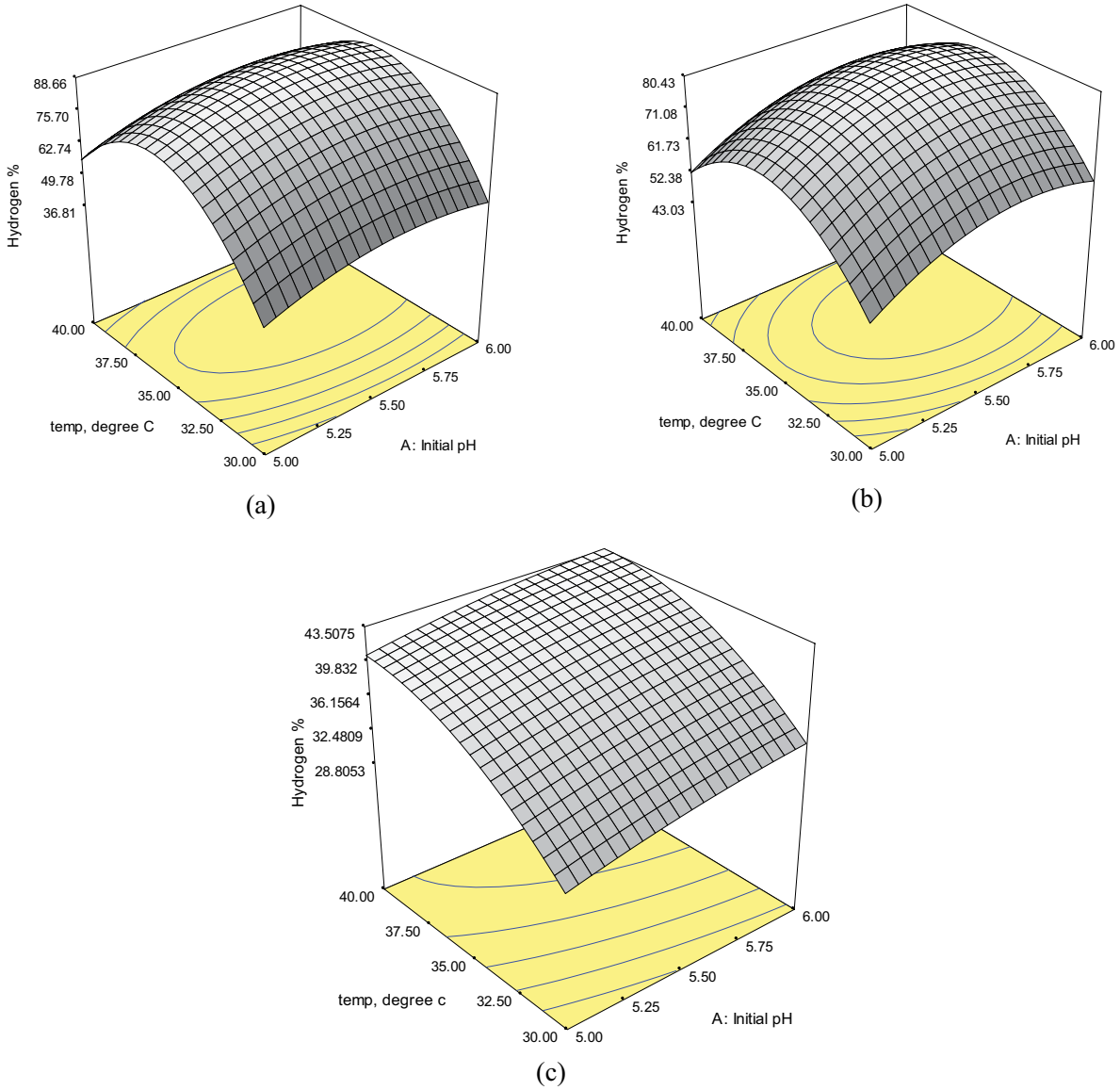

Fig. 3. Three-dimensional and contour plots of hydrogen percentage at (a) 24 h, (b) 16 h, and (c) 8 h.

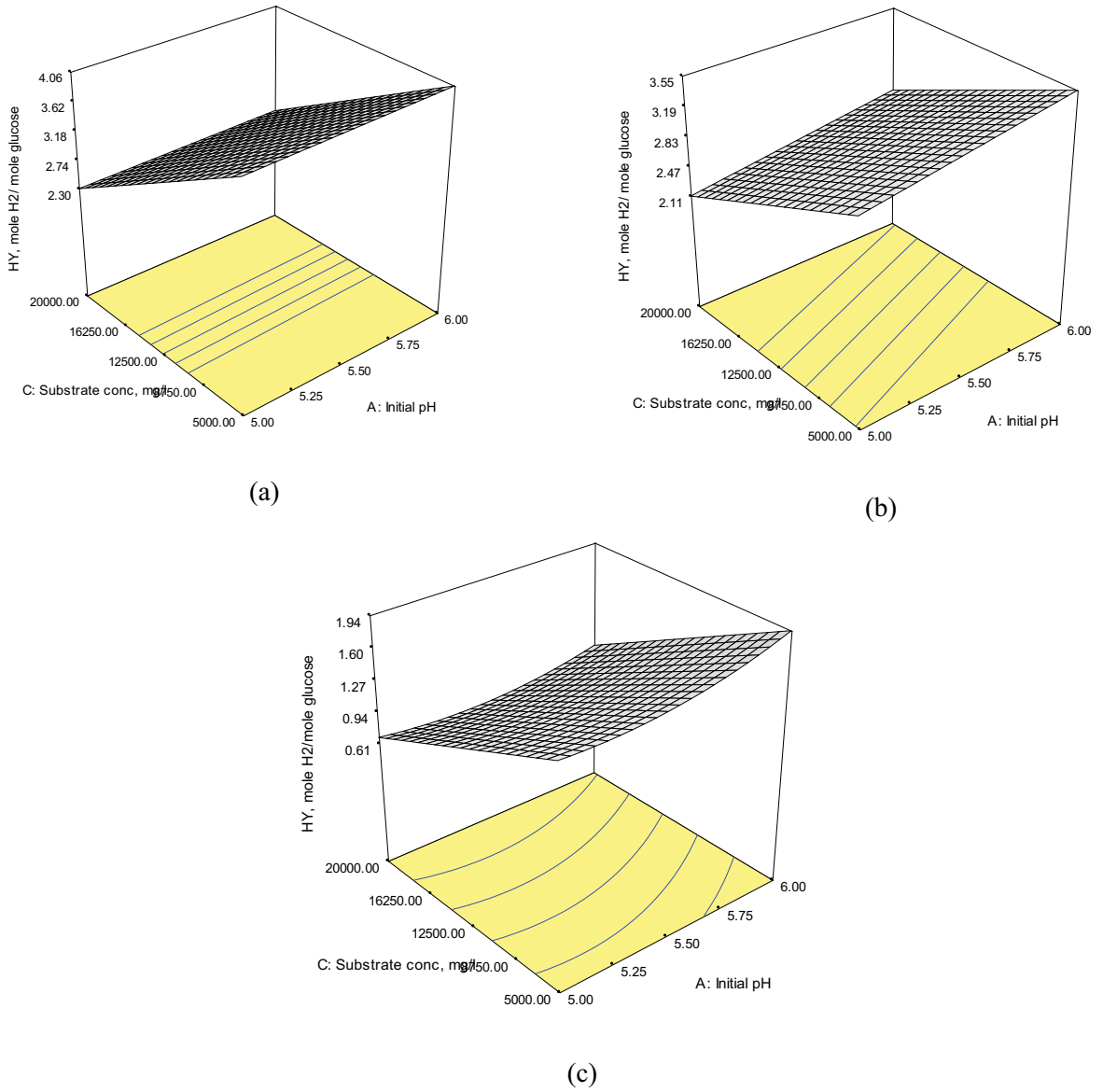

Fig. 4. Three-dimensional and contour plots of hydrogen yield at (a) 24 h, (b) 16 h, and (c) 8 h.

at the lowest substrate concentration of 5,000 mg L^{-1}, at the highest pH and the lowest substrate concentration (Fig. 4). It seems that at higher substrate concentrations organic acids accumulate which results in pH drop and might stop the metabolism of the HPB bacteria. Further, when the microorganism concentration is low, there would be insufficient bacterial cells to stabilize the organic acid production by fermentative organisms, which leads to a lower response. Therefore, pH and POME concentration are considered as two significant parameters on HY.

3.3. Biohydrogen production kinetic

To describe the performance of biological processes, modeling is of great importance. Understanding the process kinetic creates a balanced base for examination and controls the process. Moreover, it can be used to control the influence of operational and environmental parameters on the substrate consumption rate as well. Hence, kinetic studies help to optimize the performance of the biological process in the reactors. There are some kinetic models such as Stover–Kincannon, Monod, first order, second order, Contois, and so on to describe the substrate removal rate [47,48]. Fig. 5 shows the data based on 1/*S*, (g L^{-1}) versus 1/*U*, g VSS/g COD obtained from Eqs. (2) and (3). Thus, the kinetic coefficients for Monod model were considered 0.261 g L^{-1} d^{-1},0.349 mg L^{-1}, and 0.83 for U_{max}, K_s, and R^2, respectively. Gnanapragasam et al. [49] using anaerobic batch reactors studied the treatment of starch wastewater and textile dyes. In their study, Monod and Haldene's models were considered as kinetic models. The correlation coefficient R^2 for the Haldane model and Monod model was found to be 0.978 and 0.882, respectively. The substrate half saturation coefficient and the maximum specific growth

rate for Monod's model was obtained in the range of 213.4–985.6 and 0.037–0.094, respectively. Ma et al. [50] using the psychrophilic anaerobic sequencing batch reactor (ASBR) digester studied the flushed dairy manure removal. This study used four microbial growth kinetic models, that is, first order (R^2 = 0.92; k = 0.43), Grau (R^2 = 0.96 μm = 0.67 day^{-1}), Monod (R^2 = 0.76; μm = 0.07 day^{-1}, K_s = 0.24g VS) and Chen and Hashimoto models (R^2 = 0.99; μm = 0.36 day^{-1}, K = 0.23). In this study, other kinetic models could not be fitted with the COD removal data at high determination coefficient (R^2). Hence, the Monod model described the batch kinetic of the COD removal efficiency with relatively high R^2 value.

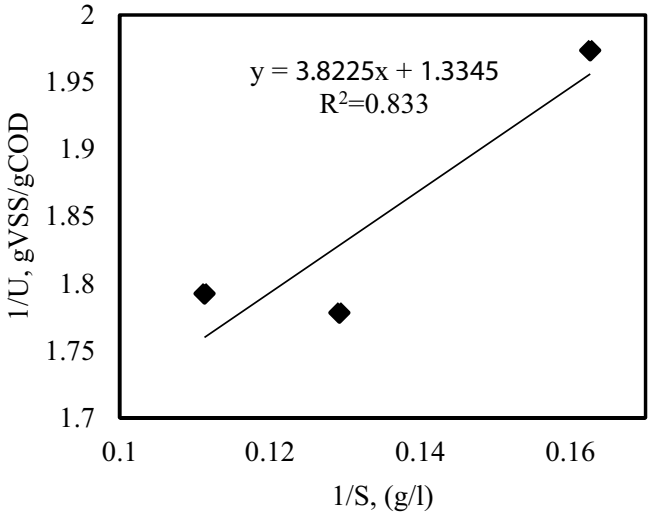

Fig. 5. Monod model.

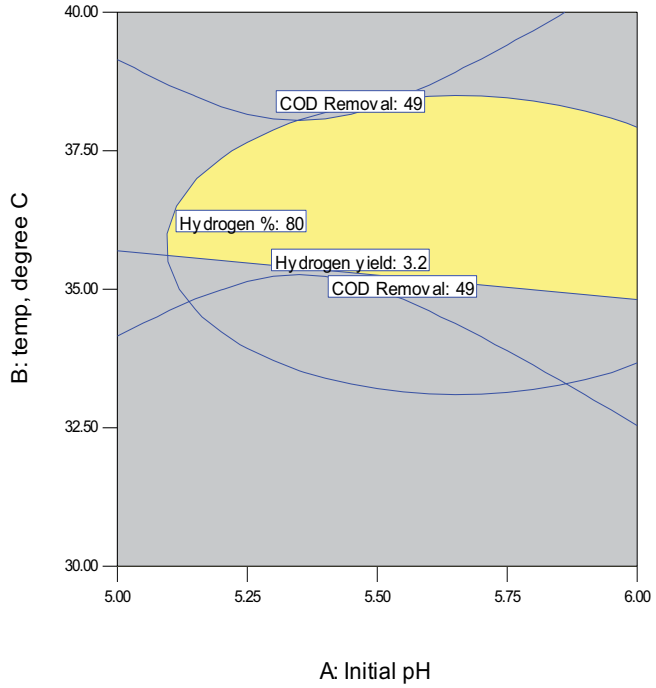

Fig. 6. Overlay plots for optimal region (a) temp vs pH.

4. Process optimization

It is required to find the regions that necessities are in agreement with critical properties the "sweet spot" for multiple responses. By overlaying critical responses on a contour plot, the appropriate compromise can be investigated visually. The overlying plot shows the possible area of the response value in the space that is defined by the factors. The space that meets the projected criteria is shown with shaded area. An overlay plot (temperature vs pH) was drawn. Fig. 6 displays the graphical optimization for the factors space, which shows the region of the achievable shaded portion. The part which fulfills the limitations is shown with yellow color, while the gray area shows the area that is not

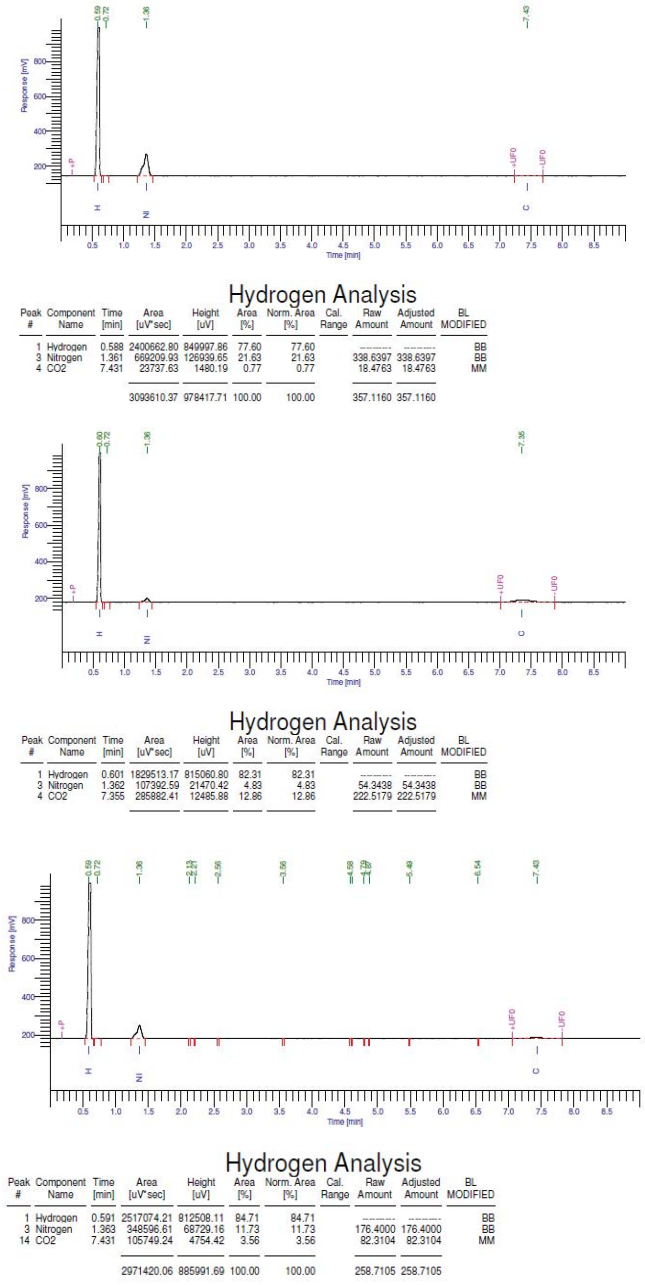

Fig. 7. GC results for optimum condition.

Table 4
Verification experiments at optimum conditions

Run	Condition		Response		
			COD removal (mg L^{-1})	Hydrogen percentage(%)	Hydrogen yield (mol H_2 mol^{-1} glucose)
1	pH = 5.2	Experimental values	46.54	77.6	2.90
	tem, °C = 37	Model values	50	81.3	3.27
	substrate conc, mg L^{-1} < 12,500	Standard deviation	±2.44	±2.61	±0.26
	ISR = 0.8				
2	pH = 5.5	Experimental values	55.26	82.31	3.52
	tem, °C = 37	Model values	49.9	80.21	3.3
	substrate conc, mg L^{-1} < 12,500	Standard deviation	±3.7	±1.48	±0.15
	ISR = 0.8				
3	pH = 6	Experimental values	59.80	84.71	3.78
	tem, °C = 37	Model values	53.21	86.73	3.33
	substrate conc, mg L^{-1} < 12.500	Standard deviation	±4.65	±1.42	±0.31
	ISR = 0.8				

in accordance with the desired criteria. The optimization criteria limit for COD removal, HY, and hydrogen percentage was selected more than 49%, 3.2 mol H_2 mol^{-1} glucose and 80%. The optimum region was found to be temperature 35°C–37°C, pH 5.3–5.9 and ISR 0.8 and substrate concentration <12,500 mg L^{-1}. To evaluate the validity of the model for highest COD removal, hydrogen percentage, and HY, the optimized reaction condition was tested experimentally. The GC results for the optimum condition are provided in Fig. 7. Moreover, to check the accuracy of the optimum condition, the standard deviation was calculated, accordingly (Table 4). From this finding, it is concluded that the optimum region could satisfy the suitable condition for achieving the highest amounts of responses.

5. Conclusion

This study was performed to assess four operational variables affect the hydrogen production from palm oil effluent in DF process. RSM was used to optimize the parameters. Among the parameters, pH and temperature were considered as significant variables. The maximum COD removal efficiency was obtained 58.32% with the corresponding variables of incubation time 24 h, pH 6 and substrate concentration of 5,000 mg L^{-1}, and a temperature of 40°C. The results of hydrogen percentage indicated that temperature and pH are influential variables on the response which was improved by increasing the variables from 42% at 8 h to 80% at 24 h. At first 8 h, maximum hydrogen percentage obtained at 39°C and pH 5.5 while over incubation time to 16 and 24 h, the highest H_2 percentage achieved in pH and temperature 5–5.5 and 36°C–38°C, respectively. Hence, increasing the temperature from 30°C to 40°C improved the H_2 percentage. The maximum HY 3.63 mol H_2 mol^{-1} glucose was obtained at the lowest substrate concentration of 5,000 mg L^{-1} (ISR 2), temperature 40°C, and incubation time 24 h. The effect of the ISRs and substrate concentration showed that the highest response could be achieved at the lowest substrate to inoculum ratio and the lowest substrate concentration, hence it was found that at higher concentrations of substrate resulted in accumulation of organic acids, therefore, when the microorganism concentration is low, there would be not sufficient bacterial cell to stabilize the organic acid production by a fermentative organism which leads to a reduction in the HY. Substrate utilization rate was modeled by Monod kinetic model and kinetic coefficients calculated as well. Monod model described the batch kinetic of the COD removal efficiency with relatively high R^2 value.

Acknowledgment

The authors gratefully acknowledge the Research Council of Malaya University for the financial support) Grant Number: ST016-2017 and RU019D-2014A).

References

[1] D. Das, T.N. Veziroğlu, Hydrogen production by biological processes: a survey of literature, Int. J. Hydrogen Energy, 26 (2001) 13–28.
[2] K. Christopher, R. Dimitrios, A review on exergy comparison of hydrogen production methods from renewable energy sources, Energy Environ. Sci., 5 (2012) 6640–6651.
[3] R. Abdallah, H. Djelal, A. Amrane, W. Sayed, F. Fourcade, T. Labasque, F. Geneste, S. Taha, D. Floner, Dark fermentative hydrogen production by anaerobic sludge growing on glucose and ammonium resulting from nitrate electroreduction, Int. J. Hydrogen Energy, 41 (2016) 5445–5455.
[4] R. Navarro, M. Sanchez-Sanchez, M. Alvarez-Galvan, F. Del Valle, J. Fierro, Hydrogen production from renewable sources: biomass and photocatalytic opportunities, Energy Environ. Sci., 2 (2009) 35–54.
[5] M.F. Awalludin, O. Sulaiman, R. Hashim, W.N.A.W. Nadhari, An overview of the oil palm industry in Malaysia and its waste utilization through thermochemical conversion, specifically via liquefaction, *Renewable* Sustainable Energy *Rev.*, 50 (2015) 1469–1484.
[6] T.Y. Wu, A.W. Mohammad, J.M. Jahim, N. Anuar, A holistic approach to managing palm oil mill effluent (POME):

biotechnological advances in the sustainable reuse of POME, Biotechnol. Adv., 27 (2009) 40–52.
[7] A. Tawfik, A. Salem, M. El-Qelish, Two stage anaerobic baffled reactors for bio-hydrogen production from municipal food waste, Bioresour. Technol., 102 (2011) 8723–8726.
[8] I. Ntaikou, G. Antonopoulou, G. Lyberatos, Biohydrogen production from biomass and wastes via dark fermentation: a review, Waste Biomass Valorization, 1 (2010) 21–39.
[9] I.C. Liu, L.M. Whang, W.J. Ren, P.Y. Lin, The effect of pH on the production of biohydrogen by clostridia: thermodynamic and metabolic considerations, Int. J. Hydrogen Energy, 36 (2011) 439–449.
[10] M. Westerholm, J. Moestedt, A. Schnürer, Biogas production through syntrophic acetate oxidation and deliberate operating strategies for improved digester performance, Appl Energy, 179 (2016) 124–135.
[11] R. Nandi, S. Sengupta, Microbial production of hydrogen: an overview, Crit. Rev. Microbiol., 24 (1998) 61–84.
[12] S.K. Khanal, W.-H. Chen, L. Li, S. Sung, Biological hydrogen production: effects of pH and intermediate products, Int. J. Hydrogen Energy, 29 (2004) 1123–1131.
[13] H.H. Fang, H. Liu, Effect of pH on hydrogen production from glucose by a mixed culture, Bioresour. Technol., 82 (2002) 87–93.
[14] A.A. Zinatizadeh, M. Mirghorayshi, P.M. Birgani, P. Mohammadi, S. Ibrahim, Influence of thermal and chemical pretreatment on structural stability of granular sludge for high-rate hydrogen production in an UASB bioreactor, Int. J. Hydrogen Energy, 42 (2017) 20512–20519, doi.org/10.1016/j.ijhydene.2017.07.029.
[15] Y. Feng, Y. Liu, Y. Zhang, Enhancement of sludge decomposition and hydrogen production from waste activated sludge in a microbial electrolysis cell with cheap electrodes, Environ. Sci.: Water Res. Technol., 1 (2015) 761–768.
[16] Y.-Y. Ning, D.-W. Jin, G.-P. Sheng, H. Harada, X.-Y. Shi, Evaluation of the stability of hydrogen production and microbial diversity by anaerobic sludge with chloroform treatment, Renewable Energy, 38 (2012) 253–257.
[17] K. Zhang, N. Ren, C. Guo, A. Wang, G. Cao, Effects of various pretreatment methods on mixed microflora to enhance biohydrogen production from corn stover hydrolysate, J. Environ. Sci., 23 (2011) 1929–1936.
[18] Y. Wong, J. Juan, A. Ting, T. Wu, High efficiency bio-hydrogen production from glucose revealed in an inoculum of heat-pretreated landfill leachate sludge, Energy, 72 (2014) 628–635.
[19] M. Cai, J. Liu, Y. Wei, Enhanced biohydrogen production from sewage sludge with alkaline pretreatment, Environ. Sci. Technol., 38 (2004) 3195–3202.
[20] A. Akhbari, A. Zinatizadeh, P. Mohammadi, M. Irandoust, Y. Mansouri, Process modeling and analysis of biological nutrients removal in an integrated RBC-AS system using response surface methodology, Chem. Eng. J., 168 (2011) 269–279.
[21] X.-J. Tang, G.-Q. He, Q.-H. Chen, X.-Y. Zhang, M.A. Ali, Medium optimization for the production of thermal stable β-glucanase by *Bacillus subtilis* ZJF-1A5 using response surface methodology, Bioresour. Technol., 93 (2004) 175–181.
[22] M. Dinarvand, M. Rezaee, M. Masomian, S.D. Jazayeri, M. Zareian, S. Abbasi, A.B. Ariff, Effect of C/N ratio and media optimization through response surface methodology on simultaneous productions of intra-and extracellular inulinase and invertase from *Aspergillus niger* ATCC 20611, BioMed Res. Int., 508968 (2013) 13.
[23] A. Ahmad, S. Ismail, S. Bhatia, Optimization of coagulation–flocculation process for palm oil mill effluent using response surface methodology, Environ. Sci. Technol., 39 (2005) 2828–2834.
[24] A. Zinatizadeh, A. Mohamed, A. Abdullah, M. Mashitah, M.H. Isa, G. Najafpour, Process modeling and analysis of palm oil mill effluent treatment in an up-flow anaerobic sludge fixed film bioreactor using response surface methodology (RSM), Water Res., 40 (2006) 3193–3208.
[25] O. Sompong, P. Prasertsan, N. Intrasungkha, S. Dhamwichukorn, N.-K. Birkeland, Optimization of simultaneous thermophilic fermentative hydrogen production and COD reduction from palm oil mill effluent by thermoanaerobacterium-rich sludge, Int. J. Hydrogen Energy, 33 (2008) 1221–1231.
[26] C.Y.L. F.Y. Chang, Biohydrogen production using an up-flow anaerobic sludge blanket reactor, Int. J. Hydrogen energy, 29 (2004) 33.
[27] A.P.H. Association, A.W.W. Association, W.P.C. Federation, W.E. Federation, Standard Methods for the Examination of Water and Wastewater, American Public Health Association, 1915.
[28] J. Fermoso, M.V. Gil, B. Arias, M.G. Plaza, C. Pevida, J. Pis, F. Rubiera, Application of response surface methodology to assess the combined effect of operating variables on high-pressure coal gasification for H_2-rich gas production, Int. J. Hydrogen Energy, 35 (2010) 1191–1204.
[29] D.C. Montgomery, C.L. Jennings, M. Kulahci, Introduction to Time Series Analysis and Forecasting, John Wiley & Sons, Hoboken, 2015.
[30] R.L. Mason, R.F. Gunst, J.L. Hess, Statistical Design and Analysis of Experiments: With Applications to Engineering and Science, John Wiley & Sons, United States, 2003.
[31] R.A. Rahman, Kinetics and Performance of Sewage Sludge Treatment Using Liquid State Bioconversion in Continuous Bioreactor, Universiti Putra Malaysia, 2009.
[32] M. Sarioglu, Ö.B. Gökçek, Treatment of automotive industry wastewater using anaerobic batch reactors: the influence of substrate/inoculum and molasses/wastewater, Process *Saf.* Environ., 102 (2016) 648–654.
[33] Y. Tao, Y. He, Y. Wu, F. Liu, X. Li, W. Zong, Z. Zhou, Characteristics of a new photosynthetic bacterial strain for hydrogen production and its application in wastewater treatment, Int. J. Hydrogen Energy, 33 (2008) 963–973.
[34] P. Mishra, S. Thakur, L. Singh, Z. Ab Wahid, M. Sakinah, Enhanced hydrogen production from palm oil mill effluent using two stage sequential dark and photo fermentation, Int. J. Hydrogen Energy, 41 (2016) 18431–18440.
[35] E. Eroğlu, U. Gündüz, M. Yücel, L. Türker, İ. Eroğlu, Photobiological hydrogen production by using olive mill wastewater as a sole substrate source, Int. J. Hydrogen Energy, 29 (2004) 163–171.
[36] F. Raposo, R. Borja, M. Martín, A. Martín, M. De la Rubia, B. Rincón, Influence of inoculum–substrate ratio on the anaerobic digestion of sunflower oil cake in batch mode: process stability and kinetic evaluation, Chem. Eng. J., 149 (2009) 70–77.
[37] S. Manickam, S. Parthasarathy, I. Alzorqi, E.H. Ng, T.J. Tiong, R.L. Gomes, A. Ali, Role of H_2 O_2 in the fluctuating patterns of COD (chemical oxygen demand) during the treatment of palm oil mill effluent (POME) using pilot scale triple frequency ultrasound cavitation reactor, Ultrasonics Sonochem., 21 (2014) 1519–1526.
[38] S.K. Leong, N.A.A. Bashah, Kinetic study on cod removal of palm oil refinery effluent by UV-Fenton, APCBEE Procedia, 3 (2012) 6–10.
[39] Z.Y. Hitit, C.Z. Lazaro, P.C. Hallenbeck, Hydrogen production by co-cultures of *Clostridium butyricum* and *Rhodospeudomonas palustris*: optimization of yield using response surface methodology, Int. J. Hydrogen Energy, 42 (2017) 6578–6589.
[40] J. Cheng, H. Su, J. Zhou, W. Song, K. Cen, Hydrogen production by mixed bacteria through dark and photo fermentation, Int. J. Hydrogen Energy, 36 (2011) 450–457.
[41] A. Reungsang, C. Sreela-or, Bio-hydrogen production from pineapple waste extract by anaerobic mixed cultures, Energies, 6 (2013) 2175–2190.
[42] M. Elsamadony, A. Tawfik, A. Danial, M. Suzuki, Use of Carica papaya enzymes for enhancement of H_2 production and degradation of glucose, protein, and lipids, Energy Procedia, 75 (2015) 975–980.
[43] Y.K. Oh, S.H. Kim, M.S. Kim, S. Park, Thermophilic biohydrogen production from glucose with trickling biofilter, Biotechnol. Bioeng., 88 (2004) 690–698.
[44] C.L. Li, H.H.P. Fang, Fermentative hydrogen production from wastewater and, solid wastes by mixed cultures, Crit. Rev. Environ. Sci. Technol., 37 (2007) 1.

[45] Z.P. Zhang, S.S. Adav, K.Y. Show, J.H. Tay, D.T. Liang, D.J. Lee, A. Su, Characteristics of rapidly formed hydrogen-producing granules and biofilms, Biotechnol. Bioeng., 101 (2008) 926–936.
[46] Y. Akutsu, Y.-Y. Li, H. Harada, H.-Q. Yu, Effects of temperature and substrate concentration on biological hydrogen production from starch, Int. J. Hydrogen Energy, 34 (2009) 2558–2566.
[47] C. Garcia, F. Molina, E. Roca, J.M. Lema, Fuzzy-based control of an anaerobic reactor treating wastewaters containing ethanol and carbohydrates, Ind. Eng. Chem. Res., 46 (2007) 6707–6715.
[48] B.K. Penumathsa, G.C. Premier, G. Kyazze, R. Dinsdale, A.J. Guwy, S. Esteves, J. Rodríguez, ADM1 can be applied to continuous bio-hydrogen production using a variable stoichiometry approach, Water Res., 42 (2008) 4379–4385.
[49] G. Gnanapragasam, M. Senthilkumar, V. Arutchelvan, T. Velayutham, S. Nagarajan, Bio-kinetic analysis on treatment of textile dye wastewater using anaerobic batch reactor, Bioresour. Technol., 102 (2011) 627–632.
[50] J. Ma, L. Yu, C. Frear, Q. Zhao, X. Li, S. Chen, Kinetics of psychrophilic anaerobic sequencing batch reactor treating flushed dairy manure, Bioresour. Technol., 131 (2013) 6–12.